

Tailoring the Adsorption Rate of Porous Chitosan and Chitosan-Carbon Nanotube Core-Shell Beads

An Ouyang,^{*ab} Ji Liang^{ab}

^a Department of Mechanical Engineering, Tsinghua University, Beijing 100084, P. R. China

^b Key Laboratory for Advanced Materials Processing Technology, Ministry of Education, Beijing 100084, P. R. China

*Corresponding author. Email: ouyangann@gmail.com.

Supporting Information

Table S1

Figure S1

Figure S2

Table S1. Initial adsorption rates of chitosan and chitosan-SWNT beads for MO and Au nanoparticles

Samples	Static Adsorption	Dynamic Adsorption		
	($\text{mg}\cdot\text{g}^{-1}\cdot\text{min}^{-1}$)	($\text{mg}\cdot\text{g}^{-1}\cdot\text{min}^{-1}$)		
	MO	MO	5 nm Au	50 nm Au
Chitosan beads	0.014	0.024	0.007	0.121
Chitosan-SWNT beads	--	0.027	0.008	0.091

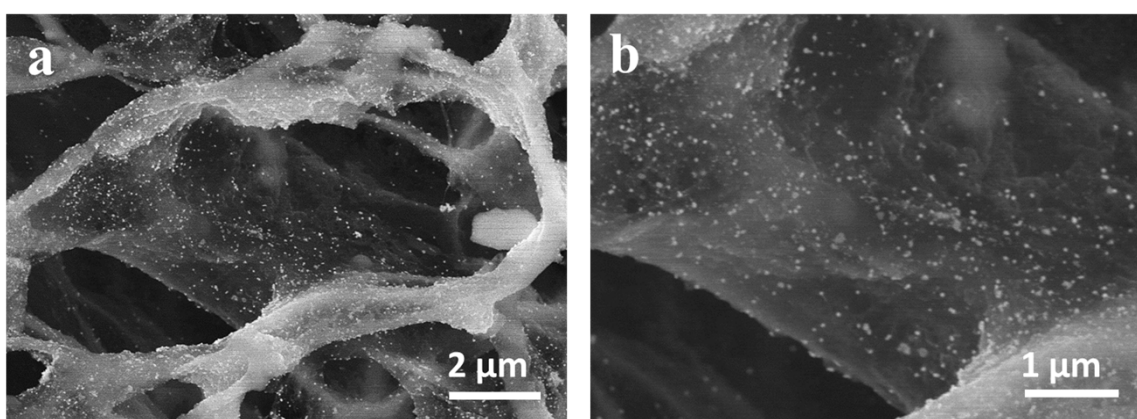


Figure S1. Characterization of chitosan beads (without a SWNT shell) after adsorption of 50 nm Au nanoparticles. a) 50 nm Au nanoparticles uniformly adsorbed on the pore walls inside the chitosan bead. b) Enlarged view showing many Au nanoparticles adsorbed on the pore walls.

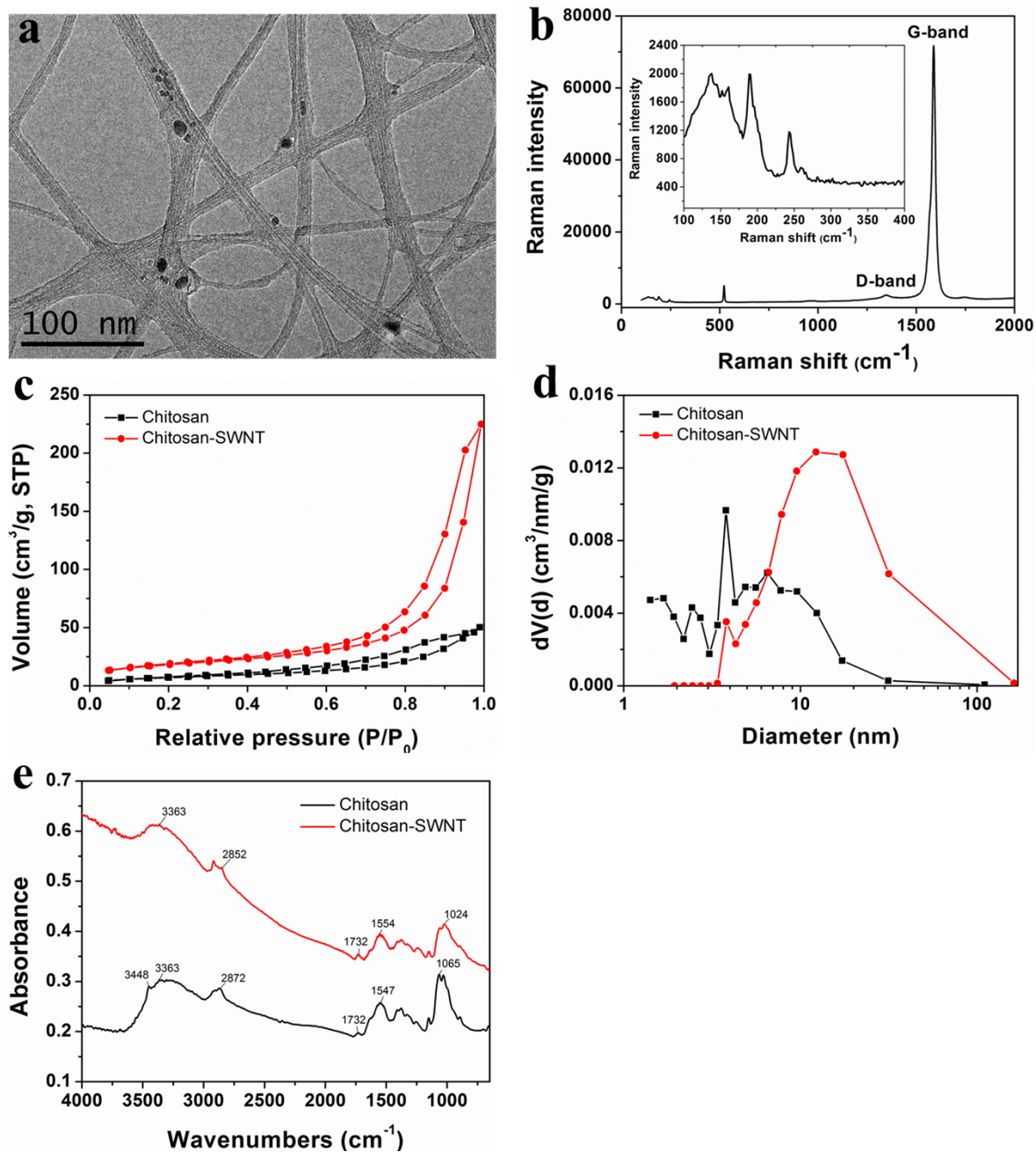


Figure S2. More characterizations on chitosan beads and SWNT films. a) High-resolution TEM image of the SWNT film after adsorption test showing interconnected single-walled nanotubes and small bundles. Black dots are adsorbed Au nanoparticles. b) Raman spectrum of the SWNT film, showing radial breathing mode peaks in 100 to 400 cm^{-1} . c) Adsorption and desorption of nitrogen isotherms of the chitosan and chitosan-SWNT beads, respectively. d) Pore diameter distribution of the chitosan and chitosan-SWNT beads, respectively. e) FTIR spectra of the chitosan and chitosan-SWNT beads.